Contribution from the Instituto de Quimica,
Universidade de Sao Paulo, Sao Paulo, Brazil

Tris(2-(aminomethyl)pyridine)iron(II): A New Spin-State Equilibrium in Solution[1]

HELENA LI CHUM,*[2a] J. A. VANIN, and MARIA ISAURA D. HOLANDA[2b]

Received May 27, 1981

The complex tris(2-(aminomethyl)pyridine)iron(II), $Fe(AMP)_3^{2+}$, is the first iron(II) system in which the high-spin form is labile that exhibits observable magnetic isomerism. Stable solutions of this complex are obtained in acetonitrile/water, methanol/water, and water solvent systems provided that there is an excess of free 2-(aminomethyl)pyridine, that the solution is at pH 8–9, and that no molecular oxygen is present. The interpretation of the solution magnetic moment measurements by the Evans method, EPR, and UV–visible absorption spectra as a function of temperature allows us to describe the spin equilibrium as $Fe(AMP)_3^{2+}$ (t_{2g}^6, $^1A_{1g}$) $\rightleftarrows$ $Fe(AMP)_3^{2+}$ ($t_{2g}^4e_g^2$, $^5A_1$). The $^5A_1$ ground state has $g = 2.01$ and is separated from the ^5E state by $\delta = 850$ cm^{-1}. Both ^5E and $^5A_1$ result from the splitting of the $^2T_{2g}$ octahedral level, and δ measures the degree of axial distortion. The separation between $^1A_1$ and ^5E at 300 K is 1100 cm^{-1}. The thermodynamic parameters for this equilibrium are $\Delta H = 5.1 \pm 0.4$ kcal/mol and $\Delta S = 17 \pm 2$ cal/(K mol) in the acetonitrile solvent system. Lower values for these parameters were found in the more polar solvents. Visible and ultraviolet absorption spectra show two intense charge-transfer bands and two weak shoulders, probably associated with d–d transitions. Ligand field parameters for these complexes have been estimated on the basis of the spectral assignments as $\Delta_{hs} = 13\,700$ cm^{-1}, $\Delta_{ls} = 18\,700$ cm^{-1}, B (Racah parameter) = 750–800 cm^{-1}, and, π (the mean electron pairing energy) = 16 100 cm^{-1}.

Introduction

The study of spin-state equilibria between low-spin (ls) and high-spin (hs) states in solution is of importance for the understanding of the role of multiplicity changes on ground- and excited-state processes, e.g., electron transfer, dissociation, and intersystem crossing of complex compounds[3,4] and some biologically important compounds.[5] Octahedral metal complexes of the first transition series of electronic configurations d^4–d^7 can display such magnetic isomerism because two electronic states of differing multiplicity may be nearly equienergetic and thermal population of the excited state is possible.[6–8]

There are more examples of iron(III) complexes than iron(II) compounds displaying spin equilibrium,[6–8] beginning with the pioneering work of Cambi and co-workers[9] on *N,N*-dialkyldithiocarbamates. A possible explanation is that synthetic difficulties associated with the presence of iron(III) impurities mask the magnetic behavior.[10]

The first well-studied iron(II) system presenting the spin-state equilibrium *in solution* was the [hydrotris(1-pyrazolyl)borato]iron(II) reported by Jesson, Trofimenko, and Eaton[11] in 1967. In 1975, Drago and co-workers[12] specially designed hexadentate ligands derived from tris(2-aminoethyl)amine and substituted pyridine-2-carboxaldehydes, which led to the obtention of two more complexes of iron(II) displaying such equilibrium in solution. The ligand field strength was properly tuned by substitution on the organic ligand. More recently, in 1978 Wilson and co-workers[13] reported the existence of the spin-state equilibrium in solution for tris[2-(2-pyridyl)imidazole]iron(II) and tris[2-(2-pyridyl)benzimidazole]iron(II). All examples related above refer to substitutionally inert complexes that display spin equilibrium in solution and spin equilibrium or spin transition[14] in the solid state.[12,15,16] In 1961, Williams et al.[17] suggested that the system tris(5,5′-dicarbethoxy-2,2′-bipyridine)iron(II) exhibits spin-state equilibrium on the basis of absorption spectra. However, no confirmation based on magnetic measurements has been published to date.

We report in this paper the first example of a well-characterized spin equilibrium *in solution* in which the high-spin form is labile that exhibits observable magnetic isomerism—the system tris(2-(aminomethyl)pyridine)iron(II) [$Fe(AMP)_3^{2+}$].[1] In the solid state, the first studies by Renovitch and Baker[18] of the temperature-dependent magnetic susceptibility indicated an anomalous behavior, which was a function of the nature of the counteranion. More recently, this system in the solid state has received special attention.[19–25] A spin transition[14] was well characterized.[19–25] The anion and the type of solvate dictate the magnetic behavior, with hydrogen bonding playing an important role. Solid–solution spin-state transition data for $[Fe_xZn_{1-x}(AMP)_3]Cl_2 \cdot C_2H_5OH$ crystals have been reported.[21] Greenaway and Sinn[22] reported magnetic properties and single-crystal structures of $[Fe(AMP)_3]Cl_2 \cdot 2H_2O$ and of the methanol monosolvate. The first compound was shown to be the low-spin facial isomer at room temperature, whereas

(1) Presented in part at the XVIII International Conference on Coordination Chemistry, Sao Paulo, Brazil, July 1977.
(2) (a) To whom correspondence should be addressed at the Solar Energy Research Institute, Golden, CO 80401. (b) Abstracted in part from the Doctoral thesis of M.I.D.H., Instituto de Quimica, Sao Paulo, Brazil, 1978.
(3) A. W. Adamson, *Adv. Chem. Ser.*, **No. 150**, 128–148 (1976).
(4) H. Taube, "Electron Transfer Reactions of Complex Compounds in Solution", Academic Press, New York, 1970; M. C. Palazzotto and H. Pignolet, *Inorg. Chem.*, **13**, 1781 (1974); H. C. Stynes and J. A. Ibers, *Inorg. Chem.*, **10**, 2304 (1971).
(5) M. Sharrock, E. Münck, P. G. Debrunner, V. Marshall, J. D. Lipscomb, and I. C. Gunsalus, *Biochemistry*, **12**, 258 (1973).
(6) E. K. Barefield, D. H. Busch, and S. M. Nelson, *Q. Rev., Chem. Soc.*, **22**, 457 (1968).
(7) R. L. Martin and A. H. White, *Transition Met. Chem. (N.Y.)*, **4**, 113 (1968).
(8) L. Sacconi, *Pure Appl. Chem.*, **27**, 161 (1971).
(9) L. Cambi and L. Szego, *Ber. Dtsch. Chem. Ges.*, **64**, 2591 (1931).
(10) (a) C. M. Harris and E. Sinn, *Inorg. Chim. Acta*, **2**, 296 (1968). (b) E. Sinn, *Inorg. Chim. Acta*, **3**, 11 (1969).
(11) J. P. Jesson, S. Trofimenko, and D. R. Eaton, *J. Am. Chem. Soc.*, **89**, 3158 (1967).
(12) M. A. Hoselton, L. J. Wilson, and R. S. Drago, *J. Am. Chem. Soc.*, **97**, 1722 (1975).
(13) K. A. Reeder, E. V. Dose, and L. J. Wilson, *Inorg. Chem.*, **17**, 1701 (1978).
(14) M. Sorai and S. Seki, *J. Phys. Chem. Solids*, **35**, 555 (1974).
(15) J. P. Jesson, J. P. Weiher, and S. Trofimenko, *J. Chem. Phys.*, **48**, 2058 (1968).
(16) R. J. Dosser, W. J. Eilbeck, A. E. Underhill, P. R. Edwards, and C. E. Johnson, *J. Chem. Soc. A*, 810 (1969); D. M. Goodgame and A. A. S. C. Machado, *Inorg. Chem.*, **8**, 2031 (1969); J. R. Sams, J. C. Scott, and T. B. Tsin, *Chem. Phys. Lett.*, **18**, 451 (1973); J. R. Sams and T. B. Tsin, *J. Chem. Soc., Dalton Trans.*, 488 (1976); J. R. Sams and T. B. Tsin, *Inorg. Chem.*, **15**, 1544 (1976).
(17) B. R. James, M. Parris, and R. J. P. Williams, *J. Chem. Soc.*, 4630 (1961).
(18) G. A. Renovitch and W. A. Baker, *J. Am. Chem. Soc.*, **89**, 6377 (1967).
(19) M. Sorai, J. Ensling, and P. Gütlich, *Chem. Phys.*, **18**, 199 (1976).
(20) M. Sorai, J. Ensling, K. M. Hasselbach, and P. Gütlich, *Chem. Phys.*, **20**, 197 (1977).
(21) (a) P. Gütlich, R. Linck, and H. G. Steinhauser, *Inorg. Chem.*, **17**, 2509 (1978). (b) P. S. Rao, A. Renveni, B. R. McGarvey, P. Ganguli, and P. Gütlich, *Inorg. Chem.*, **20**, 204–207 (1981).
(22) A. M. Greenaway and E. Sinn, *J. Am. Chem. Soc.*, **100**, 8080 (1978).
(23) B. A. Katz and C. E. Strouse, *J. Am. Chem. Soc.*, **101**, 6214 (1979).
(24) B. A. Katz and C. E. Strouse, *Inorg. Chem.*, **19**, 658 (1980).
(25) (a) A. M. Mikami, M. Konno, and Y. Saito, paper presented at Symposium on Molecular Structure, Oct 14, 1978, Hiroshima, Japan; (b) A. M. Greenaway, C. J. O'Connor, A. Schrock, and E. Sinn, *Inorg. Chem.*, **18**, 2692 (1979).

0020-1669/82/1321-1146$01.25/0

the methanol solvate was shown to be the high-spin meridional isomer at room temperature. The meridional compound underwent transition to low spin in the 100–200 K region. The methanol solvate was further investigated by Katz and Strouse,[23] who were able to elegantly show the molecular transformations in the solid state by crystallographically resolving the spin isomers. More recently,[24] these authors have shown that $[Fe(AMP)_3]I_2$ exists at room temperature in the solid state as both high-spin meridional and high-spin and low-spin facial isomers in equilibrium.

Experimental Section

Materials. Anhydrous $FeCl_2$ (Alfa Ventron) or $FeSO_4 \cdot 7H_2O$ (Baker p.a.) was used in the syntheses. Reagent grade pyridine-2-carboxaldehyde from Aldrich was freshly vacuum distilled before use. All other reagents were reagent grade, and all of the organic solvents utilized were spectroscopic grade (Merck) and were used without further purification.

Syntheses. All syntheses were carried out under a purified nitrogen atmosphere by using the Schlenk-type technique inside a glovebag. In the solid state, all compounds were kept under nitrogen or under vacuum.

Tris(2-(aminomethyl)pyridine)iron(II) Perchlorate, $[Fe(AMP)_3](ClO_4)_2$. To a solution of 0.30 g (1.1 mmol) of $FeSO_4 \cdot 7H_2O$ in 2.5 mL of 1 N HCl was added 1.5 mL of 2-(aminomethyl)pyridine (AMP) and the mixture was stirred. After 30 min at room temperature, 5 mL of 2 M $NaClO_4$ was added. A brown precipitate was readily obtained. After 2 h the solid was filtered off and rinsed with diluted $NaClO_4$ solutions and water. After drying in vacuo over P_2O_5 for 3 h, the product was purified by dissolution in a minimum amount of acetone and precipitation by addition of 5 mL of 2 M $NaClO_4$, following the same procedure described above; yield 0.4 g of a brown solid (65%).

Tris(2-(aminomethyl)pyridine)iron(II) Hexafluorophosphate, $[Fe(AMP)_3](PF_6)_2$. A procedure analogous to that for the synthesis of the perchlorate compound described above was used. Two-molar solutions of $NaPF_6$ were used to precipitate off the complex compound, obtained in 60% yield.

Tris(2-(aminomethyl)pyridine)iron(II) Chloride Acetone Solvate, $[Fe(AMP)_3]Cl_2 \cdot CH_3COCH_3$. To a solution of 15 mL of acetone and 10 mL of triethyl orthoformate was added 0.3 g (2.4 mmol) of $FeCl_2$ with vigorous stirring. After the ferrous solution stood for about 40 min, 1.2 mL (11.6 mmol) of AMP was added rapidly. After 1 h, the product was filtered off, washed with acetone, and dried in vacuo over P_2O_5 for 3 h. The product was recrystallized from acetone, collected by filtration after 1 h, washed with acetone, and dried in vacuo over P_2O_5; yield 0.6 g (50%). A similar synthesis was published in the literature for the ethanol solvate.[20]

Tris(2-(aminomethyl)pyridine)iron(II) Bromide Ethanol Solvate, $[Fe(AMP)_3]Br_2 \cdot C_2H_5OH$. This complex was synthesized by a modification of the preparation described by Sutton.[26] A solution of 0.8 g (9.2 mmol) of LiBr in 4 mL of anhydrous ethanol was added to a stirred solution of 0.32 g (2.5 mmol) of $FeCl_2$ in 10 mL of anhydrous ethanol. After the solution was stirred for about 1 h, 1.2 mL (11.6 mmol) of AMP was added rapidly. After 1 h, the product was filtered off, rinsed with ethanol, and dried in vacuo over P_2O_5 for 3 h. The product was recrystallized from ethanol, collected by filtration, washed with ethanol, and dried in vacuo over P_2O_5; yield 0.5 g (50%).

Physical Measurements. Magnetic susceptibility measurements in solution were performed by the Evans ^1H NMR method[27] with a copper–constantan thermocouple or methanol for temperature calibration. The measurements were corrected for changes in solvent density and sample concentration in the studied temperature range.[28] So that possible complication in the analysis of the Evans method arising from specific solvent–solute interactions could be avoided, the splittings of the resonances due to solvent and the inert reference Me_4Si were compared. Splitting resonances for the methyl protons in acetonitrile were within the experimental error (0.5%) identical with those for Me_4Si. On the other hand, splitting resonances due to water protons were 10% smaller than those for acetonitrile or Me_4Si. Therefore, acetonitrile was used as an inert reference. The NMR spectra were run at 100 MHz on JEOL JNM-FX100 and Varian XL-100 instruments. In the first one, the temperature was kept constant within ±0.5 to ±1 °C whereas, in the second, a four times larger temperature fluctuation was observed.

EPR spectra were obtained on an EPR spectrometer (Varian E-4) equipped with a variable-temperature controller. Quartz flat cells (S812; J. Scalon, Solvang, CA) with ground-glass joints were used.

UV–vis spectra were run on a Zeiss DMR-10 instrument, equipped with a thermostated cell holder for seven spectrophotometric cells, connected to the Lauda Brinkmann K-2/R thermostatic circulator. The temperature was measured by means of a quartz thermometer (Hewlett-Packard 2801 A) immersed in a spectrophotometric cell. For the variable-temperature measurements, an all-quartz fused cell (Hellma QI) was employed. At temperatures below 10 °C, dry nitrogen was blown into the cell compartment. Reported temperatures are ±0.5 °C.

A Metrohm E-512 or an Orion Research digital pH meter Model 801 was used to adjust the pH of the studied solutions.

In order to ensure that no decomposition of the samples occurs at high temperatures, the NMR, EPR, and UV–vis spectra were recorded first at room temperature and then at a higher temperature. After that, the sample was cooled off to room temperature and a new spectrum recorded. High-temperature data were disregarded if the measurements at room temperature did not agree within the experimental error. New spectra were then obtained with freshly prepared samples.

Stable Solutions of Tris(2-(aminomethyl)pyridine)iron(II) in Aqueous and Nonaqueous Solutions for Physical Measurements. In order to obtain solutions of $Fe(AMP)_3^{2+}$ stable for periods of 3–24 h in aqueous or mixed solvents (acetonitrile/water, methanol/water) in the studied temperature range (228–346 K), the complex was dissolved in oxygen-free solvent, containing an excess of free ligand (≥50 times the complex concentration) in the pH range 8–9 (at 20 °C).

The major solvent used throughout this work for the magnetic measurements (NMR or EPR) or absorption spectra in the 500–900-nm range was a mixture of acetonitrile (76.1% w/w), 2-(aminomethyl)pyridine (11.0% w/w), and 1 N HCl (12.9% w/w) for 0.017 M $Fe(AMP)_3^{2+}$ solutions. The preparation of the solutions for the NMR measurements, run on the JNM-FX100 spectrometer, was carried out under an argon atmosphere in a drybox (Vacuum Atmospheres Co.) fitted with a purification system (Vacuum Atmospheres Co. Model HE-493 Dri-Train). The NMR tubes (Wilmad 528-PP and coaxial 520-3) were filled and capped in the drybox prior to the transfer to the spectrometer. Other solutions were prepared by using the Schlenk-type technique inside a glovebag under nitrogen. For UV–vis spectral measurements, the complex concentration was of the order of 10^{-4} M, and the free ligand concentration was 50–100 times larger than that of the complex, at the pH range 8–9. If the pH was not kept within this range, the yellow-brown solutions turned colorless if the pH < 8 (due to acid-catalyzed dissociation)[29] or dark brown if the pH > 9, with the precipitation of insoluble material.

Influence of Molecular Oxygen. In the presence of molecular oxygen a complex autoxidation reaction takes place both in the solid state and in solution. The complex bis[2-[[(2-pyridylmethylene)amino]-methyl]pyridine]iron(II), $Fe(PP)_2^{2+}$, was isolated as the perchlorate salt in 25% yield as one of the products of the reaction in solution.

This reaction seems to proceed via the oxidation of the coordinated aminomethyl group to the corresponding imine. The resulting diimine exchanges ammonia for 2-(aminomethyl)pyridine, yielding $Fe(PP)_2^{2+}$ in a reaction similar to that described by some of us in the system iron(II)–pyruvate–2-(aminomethyl)pyridine.[30]

Diamagnetic Corrections. The following diamagnetic corrections were used: $\chi_M = -70 \times 10^{-6}$ cgsu for 2-(aminomethyl)pyridine and $\chi_M = -25 \times 10^{-6}$ cgsu for the acetonitrile/water/2-(aminomethyl)-pyridine mixed solvent, estimated from Pascal's constants[31] and from the Wiedemann additivity law.[27]

Paramagnetic Impurities. The perchlorate of tris(2-(aminomethyl)pyridine)iron(II) yielded smaller values of magnetic moments at any given temperature, compared to hexafluorophosphate, chloride,

(26) D. Sutton, *Aust. J. Chem.*, **14**, 550 (1962).
(27) D. F. Evans, *J. Chem. Soc.*, 2037 (1959).
(28) D. Ostfield and I. A. Cohen, *J. Chem. Educ.*, **49**, 829 (1972).
(29) P. Krunholz, *Struct. Bonding (Berlin)*, **9**, 139 (1971).
(30) M. I. D. Holanda, P. Krumholz, and H. L. Chum, *Inorg. Chem.*, **15**, 890 (1976).
(31) J. A. Pople, W. G. Schneider, and H. J. Bernstein, "High-Resolution Nuclear Magnetic Resonance", McGraw-Hill, New York, 1959, p 18.

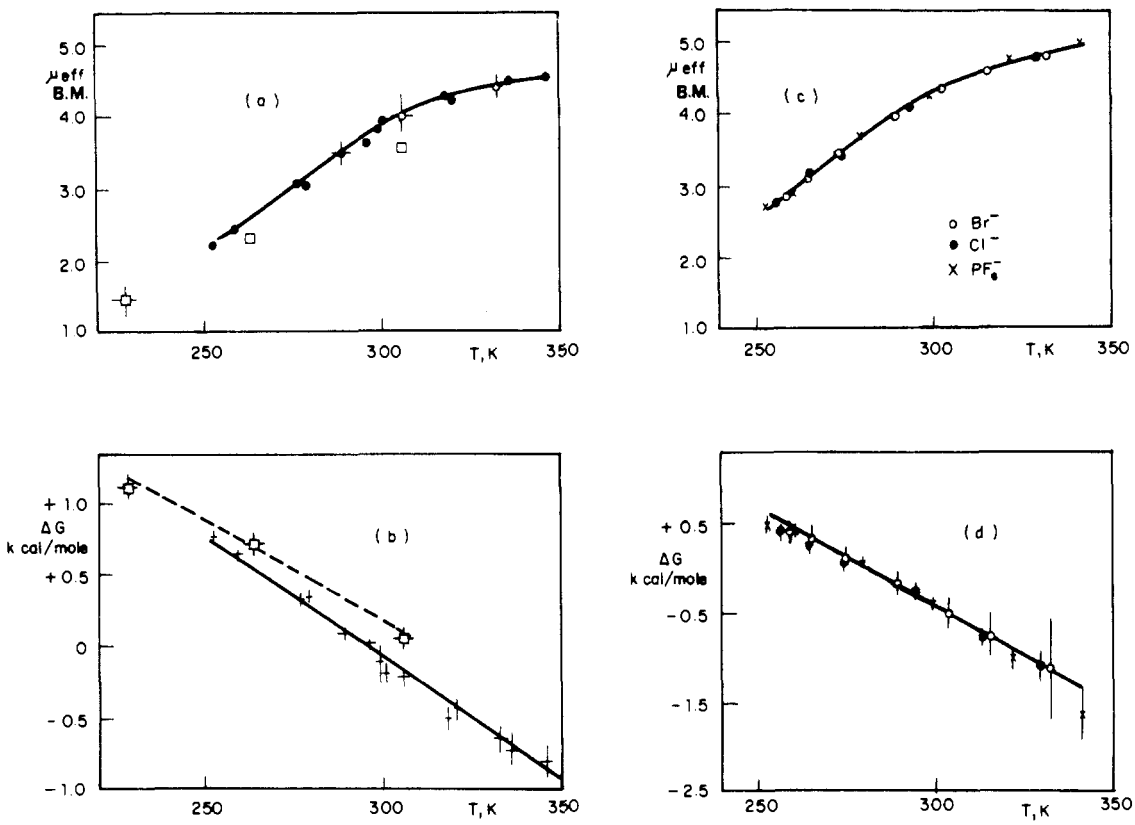

Figure 1. Solution-state magnetic moments of the system tris(2-(aminomethyl)pyridine)iron(II) as a function of temperature, solvent system, and counteranion: (a) perchlorate salt in the solvent systems acetonitrile/water/2-(aminomethyl)pyridine and methanol/water/2-(aminomethyl)pyridine; (c) bromide, chloride, and hexafluorophosphate in the acetonitrile/water/2-(aminomethyl)pyridine system. Molar free energy of the spin-state equilibrium as a function of temperature: (b) same experimental conditions as in part a; (d) same experimental conditions as in part c.

and bromide salts. The difference at room temperature (0.3 μ_B) is consistent with the three latter salts containing at most 1% of iron(III) replacing iron(II).[10b] The bromide salt was the most impure magnetic sample prepared.

Results and Discussion

Magnetic Susceptibility Data in Solution and Thermodynamic Considerations. Since in a spin-equilibrium process, both high-spin and low-spin electronic states will be thermally populated [e.g., for Fe(II) octahedral or pseudooctahedral complexes, the available electronic states will be $^1A_{1g}$ (t_{2g}^6) and $^5T_{2g}$ ($t_{2g}^4e_g^2$)], the resulting magnetic moments will be a Boltzmann distribution function of temperature. At low temperatures, the observed magnetic moments should fall in the region of 0–0.5 μ_B due to the temperature-independent residual paramagnetism of the $^1A_{1g}$ term, which arises from second-order interactions.[10b,32] At high temperatures, the observed magnetic moments should fall in the 4.8–5.5 μ_B range due to the paramagnetism of the $^5T_{2g}$ term, and the value depends on the relative importance of spin–orbit coupling, Zeeman effects, symmetry distortion, etc.[32,33] At intermediate temperatures, the observed magnetic moments fall between these limits, and an S-shaped curve of the magnetic moments vs. temperature plot is obtained. Figure 1a,c displays the non-Curie magnetic behavior observed for $Fe(AMP)_3^{2+}$ ions from CH_3CN/H_2O/AMP solutions of the perchlorate (Figure 1a) or hexafluorophosphate, chloride, and bromide (Figure 1c) salts. Figure 1a also illustrates that the same general trend is observed for the perchlorate salt in methanol/H_2O/AMP solution. At all studied temperatures the observed magnetic moments for $Fe(AMP)_3^{2+}$ fall between the low-spin ($S = 0$) and the high-spin ($S = 2$) limits. This trend is similar to that found in other spin equilibria in solution involving iron(II) complexes.[11-13] This trend, along with spectral and EPR evidence (vide infra), firmly establishes the existence of a thermal spin equilibrium

$$Fe(AMP)_3^{2+}\ (t_{2g}^6) \rightleftarrows Fe(AMP)_3^{2+}\ (t_{2g}^4e_g^2) \qquad (1)$$

The magnetic moments allow us to obtain the thermodynamic parameters for this equilibrium[12,13]

$$K_{eq} = m_{hs}/m_{ls} = (\mu_{exptl}^2 - \mu_{ls}^2)/(\mu_{hs}^2 - \mu_{exptl}^2) \qquad (2)$$

where m is the mole fraction of the spin isomer and μ_s and μ_{hs} are the effective magnetic moments for the low-spin and high-spin forms. The values of 0 and 5.2 μ_B, respectively, were assumed in this work. Since the range of temperatures employed is limited to those above 250 K, where μ_{eff}(exptl) > 2 μ_B, the use of $\mu_{ls} = 0$ does not introduce significant error in K_{eq}, within the experimental error in μ_{exptl}. An explanation of the high-spin value assumed will be given in the theoretical interpretation of the μ_{eff} vs. T curves. The thermodynamic parameters ΔH and ΔS were obtained from linear plots of the molar free energy vs. T, shown in Figure 1b,d. The thermodynamic parameters for this equilibrium are assembled in Table I, together with the values for the other spin-state equilibria in iron(II) systems in solution.

Inspection of the data in Table I indicates that ΔH and ΔS vary slightly with the solvent system employed.[34] The values

(32) J. S. Griffith, "The Theory of Transition Metal Ions", Cambridge University Press, New York, 1961.
(33) E. Konig and A. S. Chakravarty, *Theor. Chim. Acta*, **9**, 151 (1967); E. Konig, A. S. Chakravarty, and K. Madeja, *ibid.*, **9**, 171 (1967).
(34) Recalculating the data of Drago et al. for the hexadentate ligand (6-Mepy)$_2$(py)tren for each of the two solvents studied, instead of averaging them out, yields the previously observed trend in ΔH and ΔS values (Table I). The more polar solvent Me_2SO leads to considerably smaller ΔH and ΔS values for the spin-state equilibrium.

Table I. Thermodynamic Parameters for Spin-State Equilibria Involving Iron(II) Complexes in Solution at 298 K

		ΔH, kcal/mol	ΔS, cal/(K mol)	ref
2-(aminomethyl)pyridine (ClO_4^- salt)	$CH_3CN/H_2O/AMP$	5.1 ± 0.3	17 ± 2	this work
	$CH_3OH/H_2O/AMP$	4.3 ± 0.4	14 ± 2	this work
	H_2O/AMP	4.3 ± 0.5	12.5 ± 2	this work
2-(aminomethyl)pyridine (Cl^-, Br^-, or PF_6^- salts)	$CH_3CN/H_2O/AMP$	5.9 ± 0.2	21 ± 2	this work
2-(2-pyridyl)benzimidazole	CH_3CN (20%)/CH_3OH	5.1 ± 0.4	22.0 ± 1.7	13
	CH_3COCH_3	4.7 ± 0.1	18.6 ± 0.5	13
2-(2-pyridyl)imidazole	CH_3CN		26.7 ± 0.7	13
	CH_3CN (20%)/CH_3OH	3.7 ± 0.2	12.6 ± 0.4	13
	CH_3COCH_3	3.8 ± 0.1	11.6 ± 0.3	13
hydrotris(1-pyrazolyl)borate	CH_3COCH_3	3.85	11.4	11
$(6\text{-Mepy})_2(py)tren$	Me_2SO and CH_3COCH_3	2.8 ± 0.4	8.5 ± 1.5	12
	CH_3COCH_3	3.6 ± 0.2	12 ± 1	
	Me_2SO	1.9 ± 0.2	6 ± 1	
$(6\text{-Mepy})(py)_2tren$	Me_2SO and CH_3COCH_3	4.6 ± 3.3	10 ± 9	12

Table II. Parameter Fits for the Spin-Equilibrium Systems

compd	a, cm^{-1}/K	$10^{-2}b$, cm^{-1}	$10^{-2}\delta$, cm^{-1}	n	$\Sigma\Delta$	$10^3\Sigma\Delta^2$
$[Fe(AMP)_3](ClO_4)_2$	−5.6 ± 0.3	28.9 ± 0.3	−9.0 ± 0.5	15	−0.26	62
$[Fe(AMP)_3]Cl_2/Br_2/(PF_6)_2$	−6.3 ± 0.3	28.8 ± 0.3	−8.0 ± 0.5	20	−0.21	25
$Fe(6\text{-Mepy})(py)_2tren$[a]	−3.6 ± 0.3	31.2 ± 0.3	−10.3 ± 0.5	7		37
$Fe(6\text{-Mepy})_2(py)tren$[a]	−2.3 ± 0.3	21.4 ± 0.3	−10.4 ± 0.5	17		533

[a] Reference 12.

of the ΔH range from 4.3 to 5.9 kcal/mol and are comparable with the literature data, principally the data of Wilson et al.[13] on the benzimidazole derivative. The source of the ΔH is the Fe–N bond length increase,[13,35] of the order of 0.15–0.2 Å,[22-25] which accompanies the transition from low to high spin, i.e., a reorganization of the inner coordination sphere. X-ray structural determinations of the solvate $Fe(AMP)_3Cl_2 \cdot C_2H_5OH$ as the meridional isomer[25] or of the methanol solvate reveal an average 0.18-Å difference between high-spin and low-spin cations. Calculations of the reorganization energy[13] yield 2–6 kcal/mol, in agreement with the experimental observed values. The more polar the solvent, the smaller the enthalpic term. As pointed out by Wilson et al.[13] for the imidazole derivatives in solution and by Sorai et al.[19,20] and Sinn et al.[25b] for the 2-(aminomethyl)pyridine derivatives in the solid state, hydrogen bonding plays an important role in these processes. Hydrogen bonding from NH_2 to the solvent explains qualitatively the observed order of equilibrium constants: $K_{CH_3CN} > K_{CH_3OH} > K_{H_2O}$ (e.g., at 298 K, 1.41 > 0.9 > 0.43). The stronger the hydrogen-bonding ability of the solvent, the more basic the remaining coordinated nitrogen. Consequently, the ligand will exhibit a stronger σ-bonding ability, which extrastabilizes both forms thermodynamically but preferentially stabilizes the low-spin form, resulting in a decrease of the equilibrium constant with increased hydrogen-bonding ability of the solvent.

The entropic term cannot be explained solely by the spin multiplicity change. It also reflects the solvent changes. The electronic contribution to the entropy change can account for $R \ln 5 = 3.2$ eu, which represents at best one-third to one-sixth of the observed entropy changes. These data indicate that changes in the second coordination sphere accompanying the spin multiplicity change must contribute to the observed entropy changes and that hydrogen bonding must also be a factor in explaining these large entropic changes.

Theoretical Interpretation of the Magnetic Susceptibility Data in Solution and EPR Data. The gradual increase of μ_{eff} with temperature in solution is attributed to the equilibrium between the two spin isomers, as expressed in eq 1, for which the ground terms are $^1A_{1g}$ and $^5T_{2g}$, if the symmetry is octahedral. However, since in 2-(aminomethyl)pyridine the two donors nitrogens are not equivalent, the symmetry of the molecule is D_3 or lower, depending on the nature of the geometric isomer present. In solution one expects both isomers, meridional and facial, to exist, with the meridional form being predominant since it is statistically favored (cf. ref 24 where in the solid state the diiodide complex shows geometric and magnetic isomerism). The analysis of the data presented here will be performed by considering only one set of high-spin and low-spin complexes. One can consider the $Fe(AMP)_3^{2+}$ ion essentially octahedral in geometry with a superimposed trigonal distortion. This distortion splits the $^5T_{2g}$ level in ^5E and $^5A_1$.

Hoselton, Wilson, and Drago[12] proposed a theoretical expression for the temperature-dependent magnetic susceptibility appropriate for such systems. This model includes the trigonal distortion and the Zeeman effect, but does not include spin–orbit coupling, and considers the orbital reduction factor unity. From a physical point of view, we admit that such approximation is not very realistic, but indeed, since the μ_{eff} vs. T curves are very insensitive to the parameters neglected, the conclusions drawn are valid. The model and details of calculations are described in the original literature.[12,36]

The expression of the magnetic susceptibility is given by

$$\chi = N\beta^2\{(250/kT + 20/3\delta)e^{-\Delta E/kT} + (40/kT - 20/3\delta)e^{-(\Delta E+\delta)/kT}\}/(1 + 5e^{-(\Delta E+\delta)/kT} + 10e^{-\Delta E/kT}) + N\alpha \quad (3)$$

where ΔE is the energy separation between $^1A_{1g}$ and the component ^5E of the $^5T_{2g}$ octahedral level and δ is the splitting of the ^5E and $^5A_1$ components of the $^5T_{2g}$ level. When δ is negative, the $^5A_1$ is the lower of the two. $N\alpha$ is the temperature-independent paramagnetism. ΔE is a linear function of temperature: $\Delta E = aT + b$. The parameters a, b, and δ were evaluated by minimizing the sum of the deviations between measured and calculated magnetic moments, $\sum\Delta$, and the sum of the squared deviations, $\sum\Delta^2$. It was found that due to the temperature range employed in the present study, variations of $N\alpha$ do not significantly affect the fitting procedure. Therefore, a reasonable value for $N\alpha$, 5.0×10^{-4} cgsu, was assumed for the calculation, on the basis of literature data for similar compounds.[10b,12]

Table II summarizes the final parameters that best fit the experimental data, which generated the curves shown in Figure

(35) E. Konig and K. J. Watson, *Chem. Phys. Lett.*, **6**, 457 (1970).
(36) M. A. Hoselton, Ph.D. Thesis, University of Illinois, Urbana, IL, 1976.

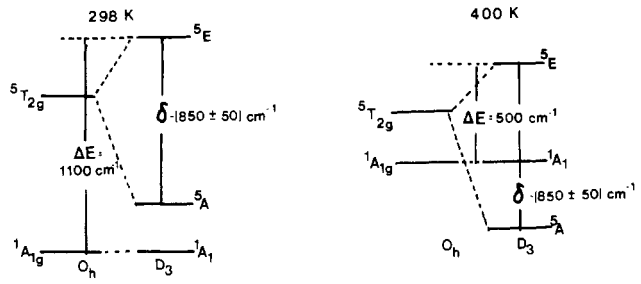

Figure 2. Energy levels of the d^6 configurations at 298 and 400 K, near the crossover.

1a,c. For comparison, the table includes the parameters for the compounds studied by Drago et al.[12]

Inspection of Table II shows that within the experimental errors, the values of the best parameters b and δ for all the salts presently studied are identical. The value of a for the ClO_4^- salt is slightly smaller than that obtained for the other salts. The difference in a values parallels the trend of ΔS observed earlier in Table I. In fact, if one expresses a values in cal/(K mol), one reproduced the ΔS values listed in Table I within the experimental error (cf. ref 35).

Figure 2 shows diagrammatically the energy levels of the ground states of $Fe(AMP)_3^{2+}$ at room temperature and at 400 K, with $\delta = -(850 \pm 50)$ cm^{-1} as obtained above (cf. ref 21). From the diagrams it is easily seen that the separation between the two ground states, $^1A_1$ and $^5A_1$, is of the order of kT, a necessary condition for the existence of the spin-state equilibrium.

A different theoretical approach proposed by Harris and Sinn[10a] considers explicitly the effective spin–orbit coupling constant and orbital reduction factors. In this model, the separation between $^1A_{1g}$ and $^5T_{2g}$ is considered constant with temperature, and another parameter C, the ratio of the vibronic partition functions of the $^1A_{1g}$ and $^5T_{2g}$ terms, is introduced (for theoretical expressions see ref 10a).

The magnetic data obtained for the $Fe(AMP)_3^{2+}$ salts, analyzed in terms of this model, produce reasonable fits, but 1 order of magnitude poorer in $\sum\Delta^2$ than fits to eq 3. As one would expect, curves are rather insensitive to variations in the spin–orbit coupling constant and orbital reduction factors. The best fits were obtained for a separation of $^1A_{1g}$ and $^5T_{2g}$ of 2.0×10^3 cm^{-1} and C of 10^{-3}, with an effective spin–orbit coupling constant $\lambda = -80$ cm^{-1} and an orbital reduction factor of $k = 0.8$, indicating some covalency. As indicated by Ewald and co-workers,[37] the parameter C must implicitly include other effects such as symmetry distortion. This fact would explain that our best fits are obtained for C values 1–2 orders of magnitude smaller than those in the literature.[10a] Therefore, symmetry distortion must be an important parameter in this case, a conclusion that is easily drawn from the application of the Drago et al.[12] model.

When taken together, these data indicate that the high-spin isomer of $Fe(AMP)_3^{2+}$ (probably in both geometric forms) is characterized by $\delta = -850$ cm^{-1}, $\lambda = -80$ cm^{-1}, and $k = 0.8$. Konig and co-workers[33] calculated the mean magnetic susceptibilities for a $^5T_{2g}$ term in axial ligand fields. For a trigonal axial field ($\delta/\lambda = 10$) and in the range of kT/λ employed in the present study (−2.13 to −2.90), μ_{eff} varied from 5.25 to 5.22 μ_B, thus justifying the use of $\mu_{hs} = 5.2 \pm 0.1$ μ_B in eq 2.

The spin equilibrium is therefore more accurately described as follows:

$$Fe(AMP)_3^{2+}\ (^1A_1) \rightleftarrows Fe(AMP)_3^{2+}\ (^5A_1) \qquad (4)$$

If, indeed, the $^5A_1$ term is the ground state of the high-spin isomer, one would expect an EPR spectrum for this compound with a g value close to 2.00 if spin–orbit coupling is not important. This expectation is confirmed in the EPR spectra of Figure 3, where $g = 2.01 \pm 0.01$. The intensity of the signal decreases with decreasing temperature, as one would expect due to the spin equilibrium (compare curves a and b in Figure 3). Therefore, the nature of the ground term of the high-spin isomer as a $^5A_1$, predicted by the theoretical analysis according to the model of Drago et al.,[12] is confirmed. The spectrum at lower temperature reveals some unresolved hyperfine structure with $a \simeq 80$ G, indicating some electron delocalization through the imine ligand (see Figure 3, curve c; the absolute intensity of curve c is 25% of that of curve a).

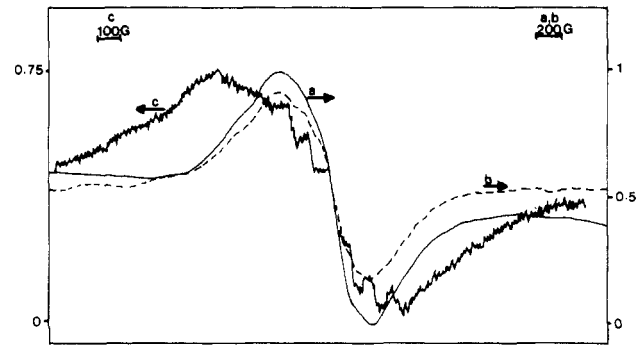

Figure 3. EPR spectra of 0.3 M perchlorate of tris(2-(aminomethyl)pyridine)iron(II) in acetonitrile/2-(aminomethyl)pyridine/water (a) at 293 K, (b) at 288 K, and (c) at 268 ± 3 K. Intensity of the spectrum at 268 K is 75% of that at 293 K.

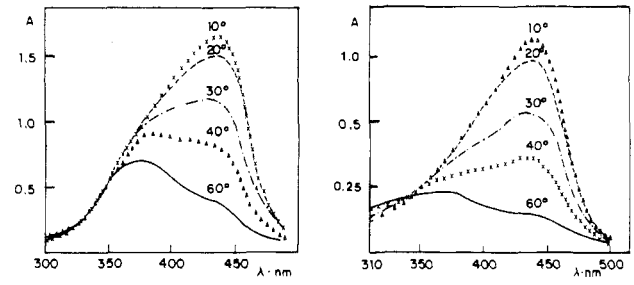

Figure 4. UV–visible absorption spectra of solutions of tris(2-(aminomethyl)pyridine) as a function of temperature: (left) 4×10^{-4} M complex concentration in acetonitrile/water/2-(aminomethyl)-pyridine; (right) 1.9×10^{-4} M complex concentration in water/2-(aminomethyl)pyridine (pH 9).

Konig, Madeja, and Watson[38] found for $Fe(bpy)_2(NCS)_2$ in the solid state a weak signal with $g \simeq 1.97$ and a partially resolved hyperfine structure with $a \simeq 90$ G. Certain other solids of the same compound gave broad spectra with $g \simeq 2.24$. Jesson et al.[11] calculated for the [hydrotris(1-pyrazolyl)borato]iron(II) a $g \simeq 2.13$ and attributed the high value to a mixture with excited states.

The EPR spectra obtained in the present work confirm the existence of the spin equilibrium by an independent technique[39] and also shed light on the nature of the ground state of the high-spin isomer.

Electronic Absorption Spectra in the 300–500-nm Range. The spin-state equilibrium is also illustrated by the absorption spectra in the region of 300–500 nm, where intense charge-transfer bands are present. Figure 4 displays examples of spectra in acetonitrile/H_2O/AMP and H_2O/AMP as a function of temperature. At 10 °C the spectrum displays an

(37) A. H. Ewald, R. L. Martin, I. G. Rose, and A. H. White, *Proc. R. Soc. London, Ser. A*, **280**, 235 (1964).

(38) E. Konig, K. Madeja, and K. J. Watson, *J. Am. Chem. Soc.*, **90**, 1146 (1968).

(39) Semiquantitative interpretation of the EPR intensities as a function of temperature agrees very well with the magnetic data, within the large experimental errors.

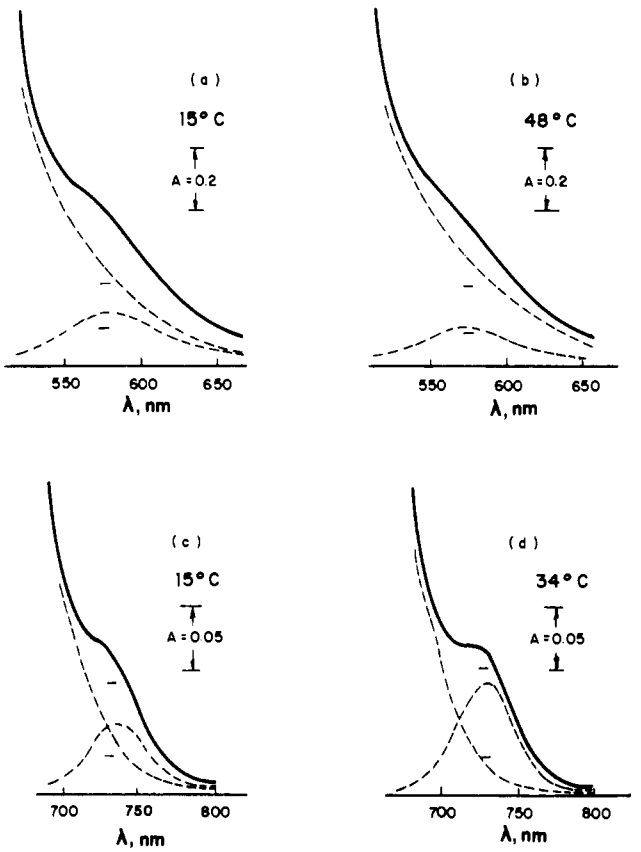

Figure 5. Absorption spectra of tris(2-(aminomethyl)pyridine)iron(II) in acetonitrile/water/2-(aminomethyl)pyridine at various concentrations (c) and temperatures: (a) $c = 2.4 \times 10^{-3}$ M at 288 K; (b) $c = 8.4 \times 10^{-3}$ M at 322 K; (c) $c = 4.2 \times 10^{-2}$ M at 288 K; (d) 4.2×10^{-2} M at 307 K. Optical paths: (a and b) 1.0 cm; (c and d) 2.0 cm.

intense band at 440 nm and a shoulder toward smaller wavelengths. As the temperature is increased, the shoulder becomes more pronounced. At 60 °C the band centered at 380 nm becomes dominant, with a shoulder at 440 nm. By decomposing these spectra into two Gaussian components, one obtains ($\delta-$ = half-width toward smaller wavenumbers): $(\lambda_{max})_{hs} = 380 \pm 5$ nm, $\delta- = (2.0 \pm 0.3) \times 10^3$ cm^{-1}, $(\lambda_{max})_{ls} = 440 \pm 5$ nm, $\delta- = (1.2 \pm 0.1) \times 10^3$ cm^{-1}, and a characteristic isosbestic point at 410 ± 5 nm for the acetonitrile solvent. In water, the three characteristic wavelengths are unchanged but the half-widths are $(1.9 \pm 0.2) \times 10^3$ cm^{-1} (380 nm) and $(0.9 \pm 0.1) \times 10^3$ cm^{-1} (440 nm), similar to those exhibited by iron diimine complexes.[29] The molar absorptivities are a marked function of temperature, increasing 1.0% per degree of decrease in temperature. At 313 K, ϵ_{hs}(380 nm) $= 3.5 \times 10^3$ M^{-1} cm^{-1} and ϵ_{ls}(440 nm) $= 4.2 \times 10^3$ M^{-1} cm^{-1}. The ratio $\epsilon_{hs}/\epsilon_{ls} = 0.83$ is constant within the experimental error in the studied temperature range. For the water solvent at 313 K, ϵ_{hs}(380 nm) $= 4.3 \times 10^3$ M^{-1} cm^{-1} and ϵ_{ls}(440 nm) $= 3.0 \times 10^3$ M^{-1} cm^{-1}, with a ratio of $\epsilon_{hs}/\epsilon_{ls} = 1.4$, constant in the studied temperature range. In fact, calculations of ΔH and ΔS based on absorption spectral data (with assumption of one absolute measurement from the Evans method to enable the calculation of the molar absorptivities) agree within the experimental error with the thermodynamic values from the magnetic data.

d–d Transitions and Ligand Field Parameters. In the 500–900-nm range, the absorption spectrum of $Fe(AMP)_3^{2+}$ in acetonitrile/water/2-(aminomethyl)pyridine displays two shoulders of low intensity, shown in Figure 5, assigned to d–d transitions. Figure 5 also shows rough decomposition of the spectra that enables us to estimate the maximum wavenumbers as $(17.2 \pm 0.5) \times 10^3$ cm^{-1} and $(13.7 \pm 0.5) \times 10^3$ cm^{-1}. Since at around 30 °C the spin-equilibrium constant is unity, the molar absorptivities are 50 ± 20 and 2 ± 1 M^{-1} cm^{-1}, respectively. The molar absorptivity of the band nearer the charge-transfer band (440 nm) depends markedly on the temperature, indicating that this transition might steal some intensity of the nearby CT band. The molar absorptivity of the lower energy band appears to be independent of temperature within the large experimental error of the decomposition procedure.

For the low-spin compound one can expect four d–d transitions (O_h microsymmetry) from the ground state $^1A_{1g}$ to the levels $^3T_{1g}$, $^3T_{2g}$, $^1T_{1g}$, and $^1T_{2g}$ in order of increasing energy.[25] Due to the high energy and the intensity of the band at 17 200 cm^{-1}, one can tentatively assign this band to the spin-allowed $^1T_{1g} \leftarrow {}^1A_{1g}$ transition. The transition $^1T_{2g} \leftarrow {}^1A_{1g}$ is probably in the 300–350-nm range[25] and therefore hidden by the intense charge-transfer bands (cf. ref 11). One cannot exclude that the band at 13 700 cm^{-1} might correspond to one of the spin-forbidden transitions of the low-spin isomer, although the intensity is relatively high (oscillator strength $f \simeq 10^{-5}$) for a spin-forbidden transition.

By using the assignments $^1T_{1g} \leftarrow {}^1A_{1g}$ (17 200 cm^{-1}) and $^3T_{2g} \leftarrow {}^1A_{1g}$ (13 700 cm^{-1}), one can calculate[40] through the Tanabe–Sugano diagrams for d^6 ions that the ligand field splitting parameter for the low-spin isomer at the equilibrium distance $\Delta_{ls} = 18\,600$ cm^{-1} and the Racah parameter $B = 750$ cm^{-1}. This B value is identical with that estimated for iron diimine complexes[29,41] and may be too small for the AMP complex, since this complex does not present such an extensive delocalization. Considering that the band at 17 200 corresponds to the $^1T_{1g} \leftarrow {}^1A_{1g}$ transition and that B values range from 800 to 900 cm^{-1}, one obtains $\Delta_{ls} = 18\,700$–$19\,200$ cm^{-1} (each value with a ±500-cm^{-1} error). Therefore, within the experimental error and the error in estimating B, $\Delta_{ls} = (19 \pm 1) \times 10^3$ cm^{-1}. In fact, if B values are in the range 750–800 cm^{-1}, the $^3T_{1g} \leftarrow {}^1A_{1g}$ transition will be at 13 700 cm^{-1}.

Energy of the Second Observable d–d Band. On the other hand, the lower energy band can be assigned to the high-spin isomer, for which one expects a $^5E_g \leftarrow {}^5T_{2g}$ transition. Examples of such transitions are seen in $Fe(H_2O)_6^{2+}$ at 10 000 cm^{-1} with $\epsilon = 1.1$ M^{-1} cm^{-1},[40] the high-spin [tris(1-pyrazolyl)borato]iron(II) at 12 500 cm^{-1} with $\epsilon = 3.2$ M^{-1} cm^{-1},[11] and some high-spin derivatives of the hexadentate ligands of Drago et al.[12] at 11 400–11 700 cm^{-1} with ϵ of 13–24 M^{-1} cm^{-1}. If the assignment of the 13 700-cm^{-1} band as the $^5E_g \leftarrow {}^5T_{2g}$ transition is correct, the ligand field splitting parameter for the high-spin isomer at the equilibrium distance, Δ_{hs}, is $(13.7 \pm 1) \times 10^3$ cm^{-1}.

Since for an octahedral complex Δ is inversely proportional to the metal–ligand distance to the fifth power, Konig and Watson[35] have found that the relationship $\Delta_{hs}/\Delta_{ls} = [R(^1A_{1g})/R(^5T_{2g})]^5$ holds for $Fe(bpy)_2(NCS)_2$, where R is the average Fe–N distance for the spin isomers. For $Fe(AMP)_3^{2+}$, the ratio $\Delta_{hs}/\Delta_{ls} = 0.72 \pm 0.09$. This ratio agrees, within the large experimental error of Δ_{hs}/Δ_{ls}, with that calculated from structural data,[21-25] $[R(^1A_{1g})/R(^5T_{2g})]^5 \sim 0.65$.

From the Tanabe–Sugano diagrams one obtains for the mean d-electron pairing energy[7] $\pi = (16 \pm 1) \times 10^3$ cm^{-1}. This value agrees very well with that obtained from Griffith's[42] approximate definition of π as $(\Delta_{hs} + \Delta_{ls})/2 = (16 \pm 2) \times 10^3$ cm^{-1}. It is also interesting to point out that another criterion for the existence of spin equilibrium, the inequality[42]

(40) B. N. Figgis, "Introduction to Ligand Fields", Interscience, New York, 1966.
(41) P. Krumholz, O. A. Serra, and M. A. DePaoli, *Inorg. Chim. Acta*, **15**, 25 (1975).
(42) J. S. Griffith, *J. Inorg. Nucl. Chem.*, **2**, 229 (1956).

$\Delta_{hs} < \pi < \Delta_{ls} = 13700 < 16000 < 19000$, is verified and that within the large experimental errors, $|\Delta - \pi|$ is of the order of 2000 cm^{-1}, another condition suggested by Griffith[42] for the existence of spin equilibrium.

Acknowledgment. We thank Professor R. A. Osteryoung for helpful discussions and Colorado State University for some of the magnetic measurements. The financial support from the Fundacão de Amparo à Pesquisa de Estado de São Paulo is gratefully acknowledged. Profitable discussions with Drs. J. H. Christie, G. Vicentini, D. Soria, W. Hatfield, and K. Sone are also acknowledged.

Registry No. $[Fe(AMP)_3](ClO_4)_2$, 64020-61-7; $[Fe(AMP)_3](PF_6)_2$, 80105-98-2; $[Fe(AMP)_3]Cl_2$, 18433-69-7; $[Fe(AMP)_3]Br_2$, 18433-70-0.

Contribution from the Chemistry Department, University of Auckland, Auckland, New Zealand, and the Research School of Chemistry, Australian National University, Canberra, Australia 2600

Spectroelectrochemical Studies of Nickel(I) Complexes: One-Electron Reduction of Nickel(II) Complexes of Dithiocarbamate and Phosphine Ligands $[Ni(R_2NCS_2)_x(Ph_2PCH_2CH_2PPh_2)_{2-x}]^{2-x}$ (x = 0, 1, 2)

GRAHAM A. BOWMAKER,[1a] PETER D. W. BOYD,*[1a] GRAEME K. CAMPBELL,[1a] JANET M. HOPE,[1b] and RAYMOND L. MARTIN[1b]

Received February 4, 1981

The electrochemical generation and stability of nickel(I) complexes of the type $[Ni(R_2NCS_2)_x(dpe)_{2-x}]^{1-x}$ (x = 0, 1, 2; dpe = $Ph_2PCH_2CH_2PPh_2$) have been investigated with use of the methods of electron spin resonance (ESR) spectroscopy and cyclic voltammetry. Reduction of the bis(dithiocarbamato) complexes $Ni^{II}(R_2NCS_2)_2$ at a Pt electrode in dichloromethane solution yields an initial planar nickel(I) species, which interconverts to a new nickel(I) species with "reversed" g values. In contrast $Ni(dpe)_2^{2+}$ undergoes two closely spaced reductions, the first of which corresponds to a nickel(I) complex with four equivalent phosphorus ligands bound to the metal. The mixed-ligand complex $[Ni^{II}(R_2NCS_2)(dpe)]PF_6$ may be reduced to a nickel(I) species with two equivalent phosphorus ligands bound to the metal. This species undergoes a series of further reactions, resulting in an overall disproportionation to $Ni^{II}(R_2NCS_2)_2$ and $Ni^0(dpe)_2$. The kinetics and mechanism of this reaction have been investigated with use of ESR spectra and cyclic voltammetry. The nickel(I) complexes $[Ni(R_2NCS_2)_2]^-$ can also be generated by γ irradiation of frozen solutions of $Ni(R_2NCS_2)_2$, and these have been characterized with use of ESR spectroscopy.

Introduction

Relatively few studies of the redox behavior of nickel(II) complexes have combined the electrochemical and electron spin resonance (ESR) spectroscopy techniques. In one such study an extensive series of complexes of nickel(II) with tetraaza macrocyclic ligands were found to undergo reversible one-electron reductions. The species produced were found to be either d^9 nickel(I) complexes or nickel(II) stabilized radical anions. These two cases were distinguished on the basis of their ESR spectra, the former having anisotropic g values greater than 2.0, the latter having isotropic g values near 2.0.[2] In one case an equilibrium between two species was detected by ESR, and this was attributed to a valence isomerization between a nickel(I) complex and the isomeric nickel(II) radical anion complex.[2b] Several of these complexes have been shown to form carbonyl adducts whose ESR spectra are different from those of the parent nickel(I) complex. The one-electron reduction of square-planar $M(mnt)_2^{2-}$ ions (M = Ni(II), Pd(II), Pt(II); mnt = maleonitriledithiolate) shows reversible behavior, and the ESR spectra of the palladium and the ^{61}Ni ($I = {}^3/_2$) enriched nickel complex are consistent with their formulation as M(I) d^9 complexes.[3,4]

A number of voltammetric studies of the redox behavior of nickel(II) dialkyldithiocarbamate complexes, $Ni(R_2NCS_2)_2$, have been reported.[5-12] In some cases there is evidence of a quasi-reversible one-electron reduction to $[Ni(R_2NCS_2)_2]^-$, although it is not yet known whether the reduction is metal- or ligand-based. $[Ni(R_2NCS_2)_2]^-$ is reported to react with 2,2′-bipyridyl to form $Ni(R_2NCS_2)(bpy)$,[11] although it has also been reported that $[Ni(R_2NCS_2)_2]^-$ reduces 2,2′-bipyridyl to the radical anion.[12]

In the present work, the techniques of voltammetry and ESR spectroscopy have been combined to study the species produced by the reduction of nickel(II) dialkyldithiocarbamate complexes of the type $Ni(R_2NCS_2)_2$ and $[Ni(R_2NCS_2)(dpe)]^+$ (dpe = 1,2-bis(diphenylphosphino)ethane). The dpe ligand was chosen because a number of relatively stable nickel(I) complexes involving this ligand have been reported previously.[13-15] The reduction of $[Ni(dpe)_2]^{2+}$ has also been studied

(1) (a) University of Auckland. (b) Australian National University.
(2) (a) Lovecchio, F. V.; Gore, E. S. *J. Am. Chem. Soc.* **1974**, *96*, 3109. (b) Gagné, R. R.; Ingle, D. M. *Ibid.* **1980**, *102*, 1444.
(3) (a) Mines, T. E.; Geiger, W. E., Jr. *Inorg. Chem.* **1973**, *12*, 1189. (b) Geiger, W. E., Jr.; Mines, T. E.; Senftleber, F. C. *Ibid.* **1975**, *14*, 2141. (c) Senftleber, F. C.; Geiger, W. E., Jr. *J. Am. Chem. Soc.* **1975**, *94*, 5018.
(4) Geiger, W. E., Jr.; Allen, C. S.; Mines, T. E.; Senftleber, F. C. *Inorg. Chem.* **1977**, *16*, 2003.
(5) Chant, R.; Hendrickson, A. R.; Martin, R. L.; Rhode, N. M. *Aust. J. Chem.* **1973**, *26*, 2533.
(6) Ahmed, M.; Magee, R. J. *Anal. Chim. Acta* **1975**, *75*, 431.
(7) Hendrickson, A. R.; Martin, R. L.; Rhode, N. M. *Inorg. Chem.* **1975**, *14*, 2980.
(8) Randle, T. H.; Cardwell, T. J.; Magee, R. J. *Aust. J. Chem.* **1976**, *29*, 1191.
(9) van der Linden, J. G. M.; Dix, A. H. *Inorg. Chim. Acta* **1979**, *35*, 65.
(10) Budnikov, G. K.; Toropova, V. F.; Ulakhovich, N. A. *Zh. Obshch. Khim.* **1974**, *44*, 492; *Chem. Abstr.* **1974**, *81*, 9093*n*.
(11) Budnikov, G. K.; Ulakhovich, N. A. *Zh. Obshch. Khim.* **1976**, *46*, 1129; *Chem. Abstr.* **1976**, *85*, 132780*u*.
(12) Budnikov, G. K.; Il'yasov, A. V.; Morozov, V.; Ulakhovich, N. A. *Russ. J. Inorg. Chem. (Engl. Transl.)* **1976**, *21*, 255.
(13) Bradley, D. C.; Hursthouse, M. B.; Smallwood, R. J.; Welch, A. J. *J. Chem. Soc., Chem. Commun.* **1972**, 872.

0020-1669/82/1321-1152$01.25/0